International Journal of Advanced Physics and Astronomy, №1 (1), 2026

IRSTI 30.51.31 https://doi.org/10.51889/IJAPA.2026.1.1.003

CONVECTIVE INSTABILITY TRIGGERED BY A DILUTE SOLID PHASE IN THE $CO_2 - Si - N_2$ GAS–AEROSOL SYSTEM AT LOW PARTICLE LOADING: A NUMERICAL STUDY

V. Mukamedenkyzy[1] and **A. Tolepbergen**[1]*

[1] *Al-Farabi Kazakh National University, Almaty, Kazakhstan*

*Corresponding Author: arsen4236@gmail.com

Received 18 May 2026; Accepted 4 June 2026

Abstract. This paper reports a numerical investigation of diffusion-convective mass transfer in the $CO_2 - Si - N_2$ gas–aerosol system at a low dispersed-phase volume fraction of $\phi = 0.5\%$ under isothermal and isobaric conditions($T = 300$ K, $p = 0.1$ MPa). Computations were carried out in ANSYS Fluent, combining the Species Transport formulation with the Eulerian Multiphase Flow framework, which together capture the coupled motion of gas components and solid microparticles with a diameter of 10 μm. The results demonstrate that even at such a low particle loading, gravitational settling of *Si* particles generates a local density inversion near the bottom wall of the upper vessel – sufficient to trigger convective instability. The mixing evolves through a sequence of well-defined stages: initial particle sedimentation, formation and subsequent breakup of a dense particle cluster, sustained downward transport through the connecting channel, and the emergence of a characteristic teardrop-shaped solid-phase structure in the lower vessel. Throughout this process, the two phases exhibit markedly different transport kinetics: CO_2 accumulates gradually and continuously, whereas Si migrates in discrete pulses, producing pronounced oscillations in the dispersed-phase volume fraction. The principal novelty of this work lies in demonstrating that Rayleigh–Taylor-type convective instability develops at $\phi = 0.5\%$ – a loading level at which any solid-phase influence on the mass transfer mechanism would not be expected a priori. This finding points to the existence of a lower concentration threshold below which the system transitions from gas–like diffusive behavior to a qualitatively different convection-driven regime. The combined Species Transport and Eulerian Multiphase approach proves capable of reproducing diffusion – convective dynamics in dilute gas–solid systems without recourse to empirical fitting parameters. The outcomes of this study are relevant to modeling aerosol particle behavior under atmospheric and industrial conditions, and may inform the design of experiments aimed at measuring mutual diffusion coefficients in gas–aerosol systems.

Keywords: gas–aerosol system, diffusion-convective mass transfer, Rayleigh–Taylor instability, dispersed phase, silicon, ANSYS Fluent, Eulerian multiphase approach, concentration-driven convection, gravitational sedimentation, Species Transport.

1. INTRODUCTION

Diffusion-convective mass transfer in gas–solid systems underpins a broad range of natural and industrial phenomena, spanning atmospheric aerosol transport, particulate emissions from combustion facilities, and mixing in chemical reactors. Many practically relevant configurations of this kind operate under isothermal and isobaric conditions, yet their dynamics remain poorly understood owing to the intricate interplay between molecular diffusion, concentration-driven gravitational convection, and inertial settling of the dispersed phase.

In isothermal multicomponent gas mixtures, a pronounced mismatch in component diffusivities can destabilize the mechanical equilibrium of the system [1, 2]. Depending on the balance between partial concentration gradients and the thermophysical properties of the mixture, regions of locally elevated or reduced density may arise [3, 4, 5], driving concentration-induced gravitational convection.

The threshold conditions for this instability admit determination by experimental means [6], through analytical treatment within Rayleigh stability theory [1, 6], or via numerical simulation [7, 8]. A systematic review of the phenomenon in gas mixtures is available in [9].

Earlier work [1, 9] addressed primarily configurations in which mixture density decreases with height – a stratification that suppresses convective perturbations. The present study turns to the opposite arrangement: an upward-directed density gradient, which gives rise to Rayleigh–Taylor convection [10]. In gas–solid systems, this instability takes on a distinctive character – the solid dispersed phase locally elevates the mixture density in the upper region, establishing a density inversion that drives the formation of descending particle jets and convective cells. While Rayleigh–Taylor dynamics have been thoroughly examined in gas–liquid and gas–gas configurations [10, 11, 12], analogous behavior in dilute gas–solid systems – where particle loading is low enough that the very onset of instability remains an open question – has received considerably less scrutiny.

A central unresolved question concerns the minimum solid-phase volume fraction ϕ at which the dispersed component begins to appreciably alter the mass transfer mechanism. In the limiting case of $\phi \to 0$, the system reduces to a binary gas mixture governed entirely by molecular diffusion. As ϕ increases, the solid phase contributes to local density stratification and interphase momentum exchange, ultimately giving rise to convective structures.

Experimental access to such processes is hindered by the optical opacity of particle-laden media, micro-scale interfacial effects, and the inherently transient nature of the phase boundary [13, 14, 15, 16]. Computational fluid dynamics offers a practical alternative, providing spatially and temporally resolved descriptions of multicomponent multiphase flows. Nevertheless, most available numerical models are tailored either to dense suspensions or rely on empirical closure terms that restrict their validity in dilute flow regimes [17, 18, 19, 20, 21].

The present work addresses this gap through a detailed CFD study of diffusion-convective mixing in the $CO_2 - Si - N_2$ gas–aerosol system at an initial solid-phase volume fraction of $\phi = 0.5\%$. The numerical framework couples the Species Transport equations – previously validated for ternary gas systems [22, 23] – with the Eulerian Multiphase Flow method, which accounts for interphase momentum exchange without invoking empirical corrections. The core objective is to establish whether such a low particle loading is capable of qualitatively altering the mass transfer regime relative to a pure gas system, and if so, to identify the governing mechanisms and the characteristic timescales of each process stage. The critical loading ϕ_{cr} marking this transition has not been systematically characterized for gas–solid systems under isothermal and isobaric conditions, and closing this gap constitutes the primary motivation of the present study.

2. METHODOLOGY

The system under study comprises two cylindrical vessels arranged vertically and connected by a narrow cylindrical channel. At the initial moment, the upper vessel contains a mixture of CO_2 gas and solid Si microparticles at a prescribed volume fraction ϕ, while the lower vessel holds pure N_2. All calculations were performed under isothermal and isobaric conditions at $T = 300$ K and $p = 0.1$ MPa. The computational domain geometry (Figure 1) reproduces the configuration employed in earlier work [22, 23]: each vessel measures 47.5 mm in height, the connecting channel is 70 mm tall with an inner diameter of 6.1 mm. All walls are treated as impermeable, adiabatic, and no-slip.

The thermophysical properties of the gas components and solid particles are listed in Table 1. The density and viscosity values of each constituent directly govern the nature of interphase interactions and the intensity of convective structures that develop during mixing. Of particular significance is the substantial density contrast between the gas phase (CO_2, N_2) and the solid Si particles

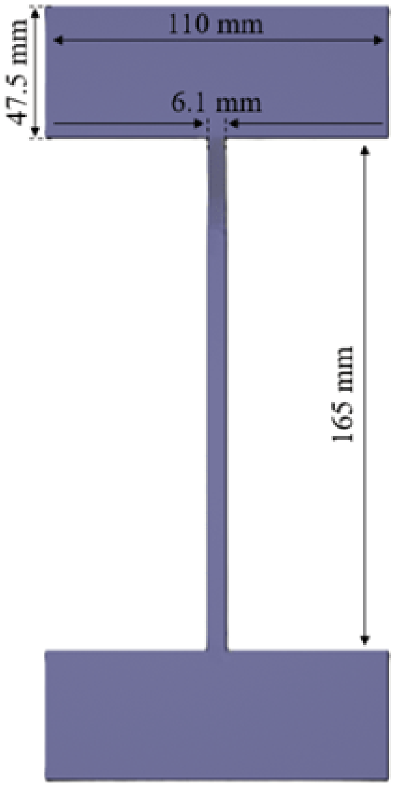

Figure 1 – Geometric model of the study area.

($\rho = 2330$ kg/m^3), which amplifies the gravitational contribution to dispersed-phase dynamics and constitutes the primary factor controlling the conditions under which density inversion occurs.

Table 1. Thermophysical properties of gases and particles.

Component	**Phase type**	**Molar mass,** g/mol	**Density,** kg/m^3	**Viscosity,** Pa·s	**Thermal cond.,** W/(m·K)	c_p, J/(kg·K)
CO_2	gas	44.01	1.977	1.48×10^{-5}	0.0166	844
Si	solid	28.09	2330	—	148.0	700
N_2	gas	28.02	1.165	1.76×10^{-5}	0.0259	1040

The computational approach builds on a gas diffusion model validated in prior work [22, 23], extended here to incorporate a solid dispersed phase. Gas-phase species transport is handled through the Species Transport equations under isothermal and isobaric conditions, with turbulence closure provided by the SST $k-\omega$ model. The solid phase is treated within the Eulerian Multiphase Flow framework, in which both the gas and solid constituents are modelled as interpenetrating continua, each carrying its own velocity, pressure, and volume fraction fields. Mass conservation for phase q is expressed through the continuity equation:

$$\frac{\partial}{\partial t}(\alpha_q\rho_q) + \nabla \cdot (\alpha_q\rho_q\vec{v}_q) = \sum_{p=1}^{n}(\dot{m}_{pq} - \dot{m}_{qp}) + S_q \tag{1}$$

where the source terms represent the phase transition rate and characterise mass exchange between phases p and q in both directions [24]. Since no phase transitions or chemical reactions occur in this configuration, these terms vanish identically.

The momentum balance for phase q takes the form:

$$\begin{aligned}\frac{\partial}{\partial t}(\alpha_q\rho_q\vec{v}_q)+\nabla\cdot(\alpha_q\rho_q\vec{v}_q\vec{v}_q)= & -\alpha_q\nabla p+\nabla\cdot\vec{\tau}_q+\alpha_q\rho_q\vec{g}\\ & +\sum_{p=1}^{n}(\vec{R}_{pq}+\dot{m}_{pq}\vec{v}_{pq}-\dot{m}_{qp}\vec{v}_{qp})\\ & +(\vec{F}_q+\vec{F}_{\mathrm{lift},q}+\vec{F}_{\mathrm{wl},q}+\vec{F}_{\mathrm{vm},q}+\vec{F}_{\mathrm{ud},q})\end{aligned} \tag{2}$$

where the stress-strain tensor, effective phase density, and body-force contributions are defined in accordance with the standard Eulerian multiphase formulation [24]. The gravitational term plays a central role in this problem: the density inversion between the particle-laden upper region and the pure gas in the lower vessel acts as the driving force behind Rayleigh–Taylor-type instability.

Interphase momentum exchange between the gas and solid phases is given by:

$$\sum_{p=1}^{n}\vec{R}_{pq}=\sum_{p=1}^{n}K_{pq}(\vec{v}_p-\vec{v}_q) \tag{3}$$

where K_{pq} is the interphase momentum transfer coefficient, evaluated from the Schiller–Naumann drag correlation for spherical particles of diameter $d_p=10^{-5}$ m.

The volume fraction of each phase is obtained by solving the transport equation:

$$\frac{1}{\rho_{rq}}\left(\frac{\partial}{\partial t}(\alpha_q\rho_q)+\nabla\cdot(\alpha_q\rho_q\vec{v}_q)\right)=\sum_{p=1}^{n}(\dot{m}_{pq}-\dot{m}_{qp}) \tag{4}$$

subject to the constraint that all phase volume fractions sum to unity.

The momentum balance for the solid phase s, accounting for particle pressure and granular stresses, reads:

$$\begin{aligned}\frac{\partial}{\partial t}(\alpha_s\rho_s\vec{v}_s)+\nabla\cdot(\alpha_s\rho_s\vec{v}_s\vec{v}_s)= & -\alpha_s\nabla p-\nabla p_s+\nabla\cdot\vec{\tau}_s+\alpha_s\rho_s\vec{g}\\ & +\sum_{l=1}^{N}(K_{ls}(\vec{v}_l-\vec{v}_s)+\dot{m}_{ls}\vec{v}_{ls}-\dot{m}_{sl}\overrightarrow{vxl}_{sl})\\ & +(\vec{F}_s+\vec{F}_{\mathrm{lift},s}+\vec{F}_{\mathrm{wl},s}+\vec{F}_{\mathrm{vm},s}+\vec{F}_{\mathrm{td},s})\end{aligned} \tag{5}$$

The rheological behaviour of the solid phase is described within the kinetic theory of granular flows. By analogy with molecular motion in a gas, the random translational velocity of particles arising from inter-particle collisions is characterised by a granular temperature Θ_s defined as one third of the mean square of the particle velocity fluctuation. This quantity governs the effective pressure, viscosity, and normal stresses of the solid phase, and accounts for the partially inelastic nature of collisions. The granular temperature is solved as an additional transport equation coupled to the solid-phase momentum balance (Equation (5)).

The initial conditions are as follows: upper vessel – a mixture of CO_2 and solid Si particles at a volume fraction of $\phi=0.5\%$; lower vessel and channel – pure N_2 ($\phi=0$).

No-slip conditions are imposed on all walls for the gas phase, and a particle adhesion condition is applied for the solid phase. Pressure and temperature are held constant throughout the domain at $p=0.1$ MPa and $T=300$ K.

All simulations were carried out in a transient formulation with a time step of 1 s over 1200 steps, covering 20 minutes of physical process time. A pressure-based coupled solver was employed, providing full pressure-velocity coupling within each iteration. Convective terms were discretised using the Second Order Upwind scheme, while pressure interpolation relied on the PRESTO! scheme, which delivers improved accuracy in the presence of body forces. Time integration was performed with a second-order implicit scheme.

The computational mesh had a structured topology comprising 164 120 cells and 165 974 nodes. The minimum cell size in the channel region was set to 0.25 mm, ensuring adequate resolution of local concentration and velocity gradients at the interphase boundaries. Convergence criteria were set to 10^{-6} for the velocity and pressure fields and 10^{-8} for species concentrations and phase volume fractions.

3. RESULTS AND DISCUSSION

Mixing in the $CO_2 - Si - N_2$ system at $\phi = 0.5\%$ is strongly non-stationary and unfolds through a succession of distinct stages that set the gas–aerosol system apart from purely gaseous mixing. Each stage is examined below on the basis of spatial distributions of the dispersed phase and temporal concentration profiles of the individual components.

Immediately after the partition is opened, Si particles initially distributed uniformly throughout the upper vessel begin to settle under gravity. By $t \approx 40 - 50$ s, virtually the entire dispersed phase has accumulated into a thin layer along the bottom wall of the upper vessel. During this interval, CO_2 starts to penetrate the lower vessel through the connecting channel, though the transfer rate remains low and consistent with a diffusion-controlled regime. The temporal profile of the CO_2 mole fraction in the lower vessel (Figure3 a) shows a slow, monotonic rise from zero to values on the order of $0.002 - 0.003$, characteristic of purely diffusive transport. The Si volume fraction in the lower vessel (Figure3 b) stays essentially at zero throughout this period, as no particles have yet reached the channel entrance. At this stage, therefore, the two phases evolve largely independently of one another – the gas diffuses while the solid sediments.

As particles accumulate along the bottom wall of the upper vessel, the local mixture density in that zone rises sharply, establishing a density inversion in which a heavier layer sits above the comparatively light gas in the lower vessel. This configuration satisfies the classical conditions for Rayleigh–Taylor instability. Around $t \approx 100 - 105$ s, a characteristic disturbance develops in the upper vessel: the dense particle cluster that has built up near the bottom wall lifts upward and subsequently breaks apart into numerous smaller fragments. On the CO_2 mole fraction profile (Figure3 a), the transition to convective transport manifests as a pronounced increase in the slope of the curve near $t \approx 100 - 105$ s. The Si volume fraction trace (Figure3 b) shows a sharp upward spike at the same moment, reflecting the impulsive entrainment of dispersed-phase fragments into convective motion. This juncture marks the crossover from diffusion-dominated to convection-dominated behaviour – a transition that occurs at $\phi = 0.5\%$ — a loading level at which any solid-phase influence would not be anticipated a priori, and which constitutes one of the principal findings of this study.

Following cluster breakup, the dispersed-phase fragments are swept into the downward convective current and begin entering the connecting channel. By $t \approx 220 - 270$ s, particle flow through the channel has reached a quasi-steady character. At this point, the CO_2 mole fraction in the lower vessel (Figure3 a) has climbed to values in the range $0.08 - 0.10$ – several times higher than would be expected from purely diffusive transport over the same time interval. The Si volume fraction (Figure3 b) over this period exhibits a series of decaying oscillations with an amplitude of approximately $0.002 - 0.003$, each peak corresponding to a discrete pulse of particles arriving through the channel. The contrast in phase kinetics at this stage is fundamental: CO_2 accumulates smoothly and continuously, whereas Si arrives in intermittent bursts tied to individual convective events.

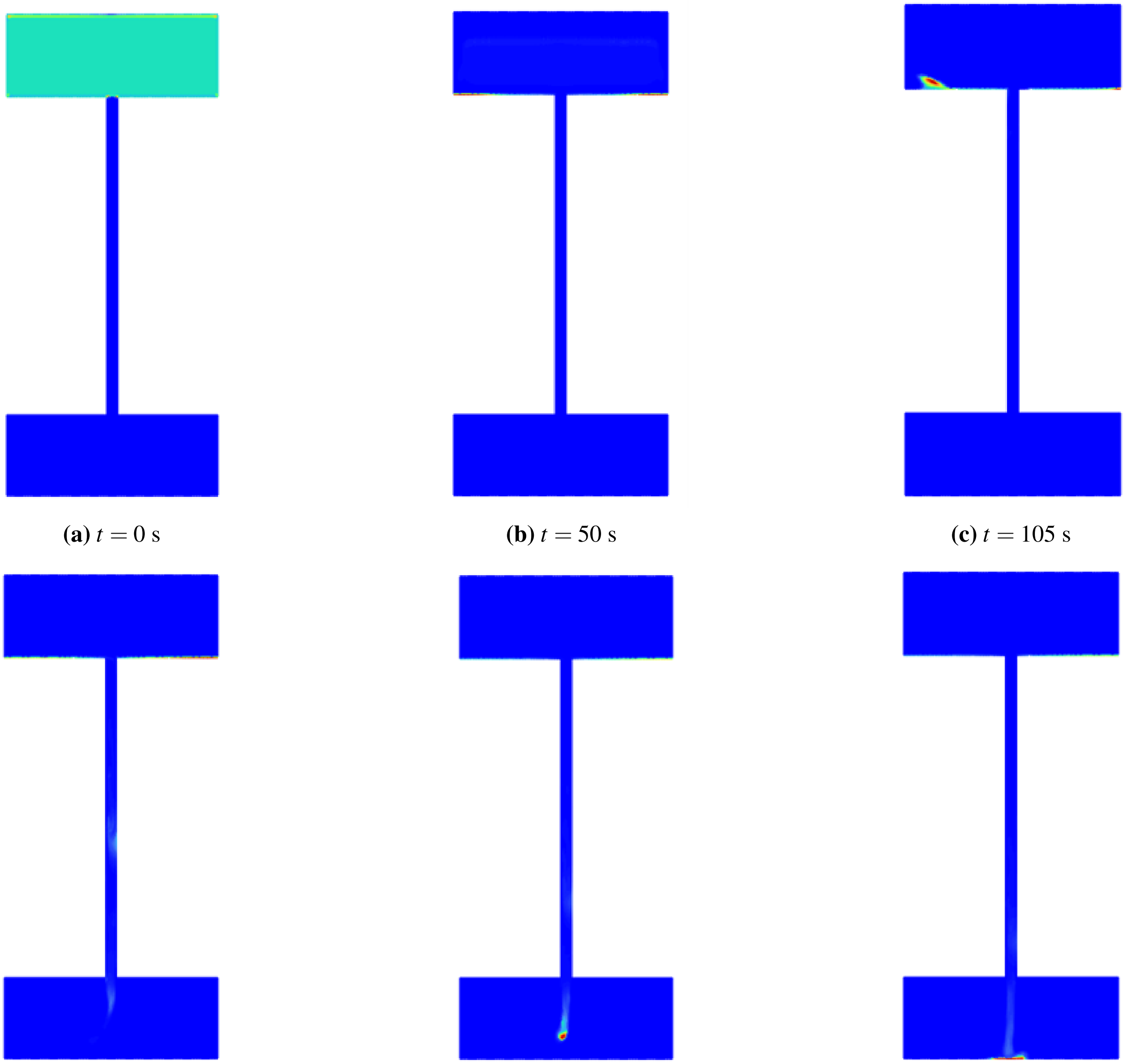

(a) $t = 0$ s **(b)** $t = 50$ s **(c)** $t = 105$ s

(d) $t = 255$ s **(e)** $t = 280$ s **(f)** $t = 300$ s

Figure 2 – Spatial distribution of the Si particle volume fraction in the $CO_2 + 0.005\,Si - N_2$ system at $p = 0.1$ MPa, $T = 300$ K at successive time instants: a) $t = 0$ s – uniform distribution of the dispersed phase throughout the upper vessel; b) $t = 50$ s – particle sedimentation onto the bottom wall of the upper vessel; c) $t = 105$ s — onset of convective disturbance and breakup of the dispersed-phase cluster; d) $t = 255$ s – downward particle flow through the connecting channel; e) $t = 280$ s – formation of a teardrop-shaped dispersed-phase structure in the lower vessel; f) $t = 300$ s – final distribution of particles along the bottom of the lower vessel.

Upon reaching the lower vessel, the particle stream consolidates into a compact teardrop-shaped structure of elevated local dispersed-phase concentration. Clearly resolved at $t \approx 280$ s (Figure 2c), this morphology represents a direct signature of Rayleigh–Taylor instability in a gas–solid medium – the solid-phase analogue of the density fingers characteristic of classical RT convection. By $t \approx 300$ s, the structure settles onto the floor of the lower vessel and spreads gradually across its surface. Beyond $t = 300$ s, both concentration profiles enter a quasi-stationary regime: the CO_2 curve (Figure 3 a) continues to rise slowly, approaching an asymptotic value of approximately $0.10 - 0.11$, while the Si trace (Figure3 b) levels off at around $0.004 - 0.005$, reflecting near-complete displacement of the dispersed phase into the lower vessel.

Taken together, these observations confirm that at $\phi = 0.5\%$ the presence of the solid dispersed phase qualitatively reshapes the mass transfer mechanism relative to a pure gas system. Particle accumulation at the bottom of the upper vessel generates sufficient local density stratification to exceed the threshold for convective instability. The two phases respond to this instability in fundamentally different ways: the gas phase undergoes a gradual, continuous acceleration in transport, whereas the solid phase migrates through a sequence of discrete impulsive events, each linked to an individual convective episode. This divergence reflects a deep asymmetry in the inertial properties of the two phases and in the way each interacts with the gravitational field.

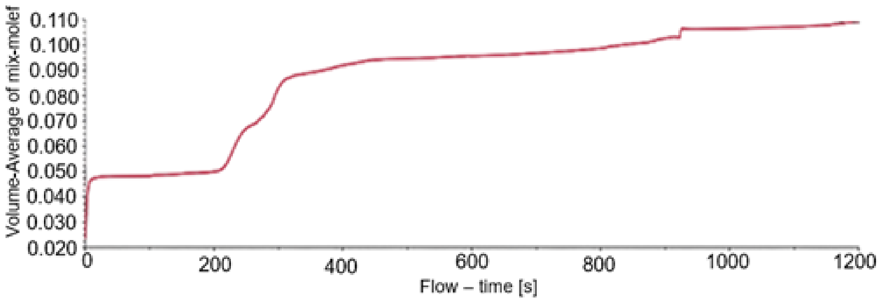

(a)

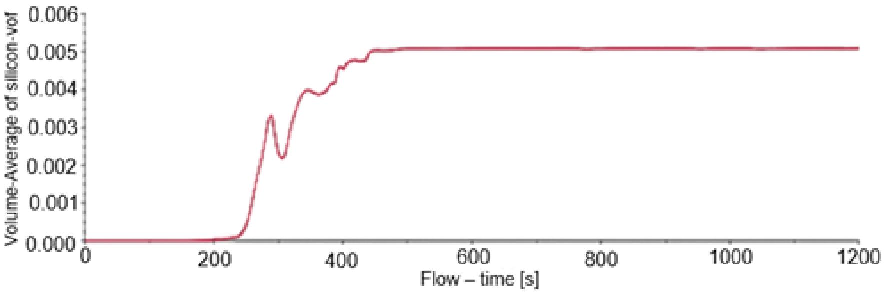

(b)

Figure 3 – Temporal evolution of gas and solid particle concentrations in the $CO_2 + 0.005\,Si - N_2$ system at $p = 0.1$ MPa and $T = 300$ K: a) CO_2 mole fraction; b) Si volume fraction.

4. CONCLUSION

This study presented a numerical investigation of diffusion-convective mass transfer in the $CO_2 - Si - N_2$ gas–aerosol system at a very low solid-phase volume fraction of $\phi = 0.5\%$ under isothermal and isobaric conditions. Simulations were conducted in ANSYS Fluent using a combined approach integrating the Species Transport equations with the Eulerian Multiphase Flow method.

The results establish that even at this low particle loading, the system behaves in a manner qualitatively distinct from a pure gas mixture. Gravitational settling of Si particles onto the bottom wall of the upper vessel produces a local density inversion that, at $t \approx 100 - 105$ s, crosses the threshold for convective instability and triggers a flow restructuring consistent with the Rayleigh–Taylor mechanism. This transition is evidenced by a sharp acceleration in CO_2 gas-phase transport and the appearance of pronounced oscillations in the Si volume fraction, indicative of intermittent, non-stationary dispersed-phase migration. The formation of a teardrop-shaped solid-phase structure in the lower vessel at $t \approx 280$ s provides morphological confirmation of the RT instability.

A key outcome of this work is the demonstration that the two phases follow fundamentally different transport pathways: CO_2 is transferred smoothly and continuously via a diffusion-convective mechanism, whereas Si migrates through a succession of discrete convective pulses. This divergence stems from a deep asymmetry in the inertial characteristics of the phases and their respective responses to the gravitational field.

The combined Species Transport and Eulerian Multiphase model proves applicable to diffusion-convective processes in dilute gas–solid systems without recourse to empirical corrections. These findings carry practical relevance for assessing conditions under which even trace concentrations of a dispersed phase can substantially alter the mass transfer regime — notably in the design of experiments targeting mutual diffusion coefficient measurements in gas–aerosol systems.

Future work should address a systematic parametric study across the range $\phi = 0 - 5\%$ to identify the critical loading ϕ_{cr} below which solid-phase effects on gas-phase transport become negligible, alongside extension of the model to three-dimensional geometry and incorporation of heat transfer effects.

REFERENCES

1. Kosov, V. N. and V. D. Seleznev. *Anomalous Occurrence of Free Gravitational Convection in Isothermal Ternary Gas Mixtures*. Ekaterinburg, Russia: Ural Branch of the Russian Academy of Sciences, 2004.
2. Dil'man, V. V., D. A. Lipatov, V. A. Lotkhov, and et al. “Instability in unsteady-state evaporation of binary solutions into an inert gas.” *Theoretical Foundations of Chemical Engineering* 39, no. 6 (2005): 566–572.
3. Kaminskii, V. A. “Special modes of three-component diffusion in gases.” *Russian Journal of Physical Chemistry A* 85, no. 12 (2011): 2203–2208.
4. Kosov, V. N., Y. I. Zhavrin, and V. D. Seleznev. “Inversion of the density gradient and the 'gate' in isothermal mixing of gases.” *Technical Physics* 43, no. 5 (1998): 488–492.
5. Zhavrin, Y. I., V. Kosov, D. Kul'zhanov, and K. Karataeva. “Effect of the pressure on the type of mixing in a three-component gas mixture containing a component possessing the properties of a real gas.” *Technical Physics Letters* 26, no. 12 (2000): 1108–1109.
6. Kosov, V. N., O. V. Fedorenko, Y. I. Zhavrin, and V. Mukamedenkyzy. “Instability of mechanical equilibrium during diffusion in a three-component gas mixture in a vertical cylinder.” *Technical Physics* 59, no. 4 (2014): 482–486.
7. Zhussanbayeva, A., V. N. Kossov, O. V. Fedorenko, and M. Zhaneli. “Instability of mechanical equilibrium and concentration convection in isothermal ternary gaseous systems.” *Physical Sciences and Technology* 9, no. 1-2 (2022): 55–61.
8. Moldabekova, M., V. Mukamedenkyzy, M. Asembayeva, and A. Tolepbergen. “Investigation of the diffusion of two gases equally diluted with different ballast gases.” *Recent Contributions to Physics* 89, no. 2 (2024): 57–61.
9. Kossov, V. N. and H. Altenbach. “Diffusion mechanisms of convective instability in liquid and gas mixtures.” *Journal of Applied Mathematics and Mechanics / ZAMM* 103, no. 11 (2023): e202300801.
10. Banerjee, A. “Rayleigh-taylor instability: A status review of experimental designs and diagnostics.” *Journal of Fluids Engineering* 142, no. 12 (2020): 120801.
11. Balachandar, S. and J. K. Eaton. “Turbulent dispersed multiphase flow.” *Annual review of fluid mechanics* 42, no. 1 (2010): 111–133.
12. Capecelatro, J. and et al. “Gas-particle dynamics in high-speed flows: A review.” *Annual Review of Fluid Mechanics* 56 (2024): 379–403.
13. Villafañe, L., A. Aliseda, S. Ceccio, P. Di Marco, N. Machicoane, and T. J. Heindel. “Experimental methods for dispersed multiphase flows.” *International Journal of Multiphase Flow* 189 (2025): 105239.
14. Yan, Y., K. Mohanarangam, W. Yang, and J. Tu. “Experimental measuring techniques for industrial-scale multiphase flow problems.” *Experimental and Computational Multiphase Flow* 6 (2024): 1–13.
15. Bolegenova, S., A. Askarova, S. Ospanova, and et al. “Technology of reducing greenhouse gas emissions.” *Physical Sciences and Technology* 11, no. 1-2 (2024): 64–75.
16. Tas-Koehler, S. and et al. “A critical analysis of drag force modelling for disperse gas-solid flows.” *Chemical Engi-*

neering Science (2021): 117007.

17. Akula, B. and D. Ranjan. “Dynamics of buoyancy-driven flows at moderately high Atwood numbers.” *Journal of Fluid Mechanics* 795 (2016): 313–355.
18. Liang, Y., K. Alkindi, K. Alzeyoudi, L. Liu, M. Ali, and N. Masmoudi. “Experimental investigation of three-dimensional Rayleigh-Taylor instability.” *Journal of Fluid Mechanics* 994 (2024): A7.
19. Liu, C., Y. Zhang, and Z. Xiao. “Unified model for Rayleigh-Taylor and Richtmyer-Meshkov fingers.” *Journal of Fluid Mechanics* 954 (2023): A13.
20. Peixoto, M. L. R., M. S. C. A. Brito, R. J. Santos, and V. J. P. Vilar. “Kinetic model implementation in raceway pond reactors.” *Chemical Engineering Research and Design* 210 (2024): 150–162.
21. Pancorbo, P. M., J. M. Ortiz de Zárate, H. Bataller, and F. Croccolo. “Gravity effects on Soret-induced fluctuations.” *European Physical Journal E* 40, no. 2 (2017): 22.
22. Kossov, V. N., V. Mukamedenkyzy, A. Tolepbergen, and H. Altenbach. “Peculiarities of combined mixing caused by instability of mechanical equilibrium.” *International Journal of Chemical Engineering* (2025): 9643371.
23. Mukamedenkyzy, V. and A. Tolepbergen. “Some features of Rayleigh-Taylor convection in the mixing of ideal gas mixtures.” *Recent Contributions to Physics* 92, no. 1 (2025): 110–119.
24. ANSYS, Inc., “ANSYS Fluent Theory Guide 2025 R1.” ANSYS Documentation, 2025, accessed: November 2025.

Information about authors

V. Mukamedenkyzy *– Candidate of Physical and Mathematical Sciences, Associate Professor of the Department of Thermal Physics and Technical Physics, Al-Farabi Kazakh National University, Almaty, Kazakhstan, email: mukamedenkyzyvenera@gmail.com,*
A. Tolepbergen *– student of Department of Thermal Physics and Technical Physics, Al-Farabi Kazakh National University, Almaty, Kazakhstan, e-mail: arsen4236@gmail.com* .